

# Oxidation of ultrafine-cemented carbide prepared from nanocrystalline WC–10Co composite powder

Xiaoliang Shi <sup>\*</sup>, Hua Yang, Gangqin Shao, Xinglong Duan, Sheng Wang

*State Key Laboratory of Advanced Technology for Materials Synthesis & Processing, Wuhan University of Technology,  
122 Luoshi Road, Wuhan 430070, China*

Received 26 April 2007; received in revised form 5 July 2007; accepted 26 July 2007  
Available online 19 August 2007

## Abstract

The oxidation behavior and associated properties, phases and microstructure of ultrafine WC–10Co-cemented carbide using WC–10Co nanocomposite powder prepared by spray pyrolysis-continuous reduction and carbonization technology, were investigated in the 450–700 °C temperature range at 50 °C intervals. The results showed that the working temperature of the cutting edge should be lower than 550 °C in air without coolant in order to assure the lifespan and working efficiency of ultrafine WC–10Co-cemented carbide materials as cutting tools.

© 2007 Elsevier Ltd and Techna Group S.r.l. All rights reserved.

**Keywords:** WC–10Co; Nanocomposite powder; Ultrafine-cemented carbide; Oxidation; Working temperature

## 1. Introduction

WC–Co cemented carbides are universally used for miniature drills for printed circuit boards, pins for dot-printers, wood machining, dental work, cutting tools, rock drill tips and other wear resistant parts due to their unique combination of hardness, toughness and strength [1–3]. Recently, ultrafine WC–Co cemented carbide with both high hardness and high strength are demonstrating their excellent potentialities [4–6]. In most circumstances, hardness directly indicates the wear resistance of tool. Thus, the harder the grade, the higher the wear resistance of the cutting edge. In cemented carbide for metal cutting purposes, the quality of a cemented carbide grade is dictated substantially by its high-temperature properties, and the lifespan and working efficiency of ultrafine WC–Co cemented carbide materials as cutting tools in air are strongly depending on its oxidation resistance.

In recent years, researchers have made concentrated efforts to study the high-temperature hardness and wear characteristics of WC–Co cemented carbide. The hardness of a simple WC–10Co-cemented carbide at 800 °C will feature only about one third of that at room temperature, whereas the specimen

containing additions of TiC and (Ta, Nb)C will feature about half of its hardness at room temperature [7]. Luyckx S [8] investigated the high-temperature hardness of WC–Co–Ru from room temperature to 900 °C in high vacuum. The data available on the high-temperature hardness of WC–Co–Ru was also found in a patent [9]. A wear test between cemented WC–Co alloy and carbon steel was conducted to observe the wear behavior of cemented WC–Co alloy at 400 °C by Marui E et al. [10]. Hegeman JBJW et al. [11] observed the micrographs of polished and heat-treated WC–10Co specimens in high vacuum with subsequent slow cooling. Acchar W et al. [12] researched the transverse rupture strength (TRS) measured in three point-bending in air at temperatures between room temperature and 1000 °C. Basu SN et al. [13] investigated the oxidation behavior of coarse WC–Co samples in flowing Ar–O<sub>2</sub> gas mixtures at 600 °C, 700 °C and 800 °C, respectively. Casas B et al. [14] studied the oxidation-induced strength degradation of WC–Co hardmetals containing different binder phases with the same carbide mean grain size (2.5 μm) at 700 °C in air.

However, the oxidation resistance of ultrafine WC–10Co-cemented carbide without additives in air is seldom touched. In this paper, an investigation was carried out to study the oxidation resistance of ultrafine WC–10Co-cemented carbide based on WC–10Co nanocomposite powder prepared by spray pyrolysis-continuous reduction and carbonization technology.

<sup>\*</sup> Corresponding author. Tel.: +86 27 87216912; fax: +86 27 87216912.

E-mail address: [sxl@mail.whut.edu.cn](mailto:sxl@mail.whut.edu.cn) (X. Shi).

The microstructure, phases and properties of the oxidized cemented carbides were investigated.

## 2. Experimental

WC–10 wt.%Co nanocomposite powder without additives, produced by spray pyrolysis-continuous reduction and carbonization [1], was used for this study. The powder was ball-milled in acetone for 48 h, and dried at 90 °C in vacuum oven. The particle size was characterized by a Brunauer–Emmet–Teller (BET) analyzer. The green compacts were consolidated in a vacuum sintering process at 1380 °C for 60 min. Sintered specimens, 25 mm × 10 mm and a thickness of 10 mm, were characterized for microstructure and grain size by a JSM-5610LV scanning electron microscopy (SEM). To investigate the oxidation behavior, differential scanning calorimetry/thermogravimetric (DSC/TG) (Netzsch STA 449C Simultaneous Thermal Analyzer) analysis was applied in air with a heating rate of 10 °C/min. Before oxidation, the sintered samples were polished with diamond pastes of 6 μm, 3 μm and 1 μm, respectively, to obtain a smooth surface. After each sequential polishing step, the surface was cleaned with acetone. Then, the samples were oxidized in the temperature range of 450–700 °C at 50 °C intervals for 4 h in muffle furnace in air with subsequent slow cooling.

The micrographs of the oxidized surface layer and specimen microstructure were investigated by SEM. The phases in the oxidized surface layer were characterized by X-ray diffraction (XRD). In order to remove the oxidized surface layer before the Vickers indentations were made, the samples were polished mechanically with emery papers down to grade 1200, and with 0.05 μm wet polishing diamond pastes, the surface was also cleaned with acetone. The Vickers hardness (3 kg) was measured at room temperature with a micro-Vickers hardness tester, and the Rockwell A hardness (HRA) (50 kg) was also measured. The TRS was measured with an MTS-810 Teststar Iis Electro-Hydraulic Servocontrolled Testing System. The Vickers hardness indentations were observed by an optical microscopy. Saturated magnetization and coercivity force were measured by a saturation induction measuring system and a förster-koerzimat 1.095, respectively.

## 3. Results and discussion

The properties of the WC–10Co nanocomposite powder are summarized in Table 1. The specific surface area of the nanocomposite powder was 5.12 m<sup>2</sup> g<sup>−1</sup> and the equivalent mean particle size was about 80 nm.

Table 1  
Properties of WC–10Co nanocomposite powder

Total carbon content [wt.%]	5.54
Free carbon content [wt.%]	0.18
Oxygen content [wt.%]	0.25
Cobalt content [wt.%]	10.08
Specific surface area [m <sup>2</sup> g <sup>−1</sup> ]	5.12

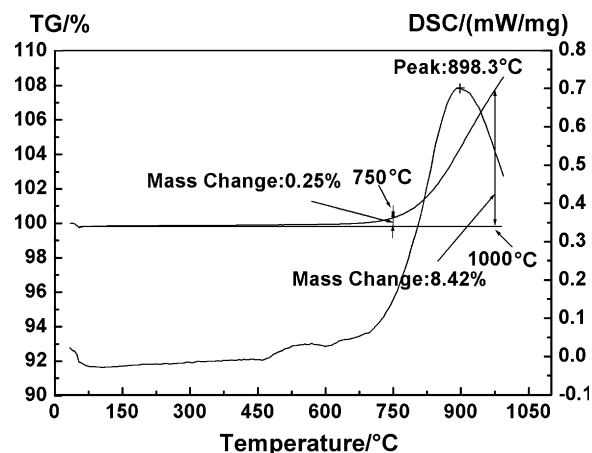


Fig. 1. DSC/TG pattern of ultrafine WC–10Co-cemented carbide from room temperature to 1000 °C in air.

The DSC/TG pattern of ultrafine WC–10Co-cemented carbide from room temperature to 1000 °C in air is shown in Fig. 1. Only one peak was observed in the DSC curve. The ultrafine WC–10Co-cemented carbide began to oxidize at about 425 °C in air. An obvious exothermic peak appeared at 898.3 °C, which can be explained by furious oxidation [15]. As shown by the TG curve, the mass increment was 0.25 wt.% from room temperature to 750 °C, which corresponds to a limited oxidation of cobalt and WC. The mass increment of 8.42 wt.% from 750 °C to 1000 °C corresponds to a prominent oxidation of Co and WC.

As shown in Fig. 2, the surface layers of WC–10Co-cemented carbide after oxidation processes at 450 °C, 500 °C, 550 °C, 600 °C, 650 °C and 700 °C, all contained WO<sub>3</sub>, Co<sub>3</sub>O<sub>4</sub> and CoWO<sub>4</sub> phases.

As shown in Fig. 3, the oxidation layer thickness was 39.1 μm, 83.1 μm, 117 μm, 619 μm, 1.25 mm and 2.12 mm, respectively. The oxide layer thickness increased with increasing oxidation temperature. When the oxidation temperature reached 700 °C, the thickness of the oxidized surface layer was 2.12 mm.

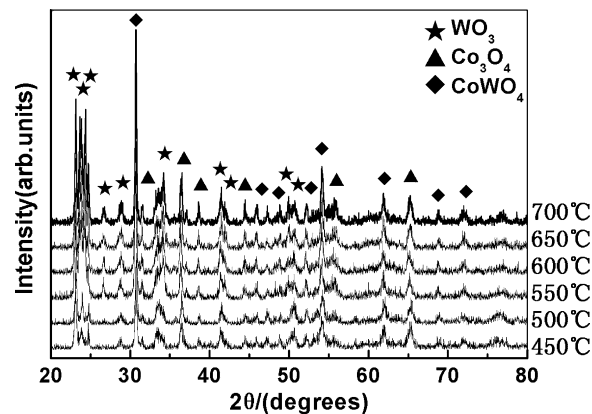


Fig. 2. XRD patterns of the surface of the ultrafine WC–10Co-cemented carbide, oxidized at different temperatures.

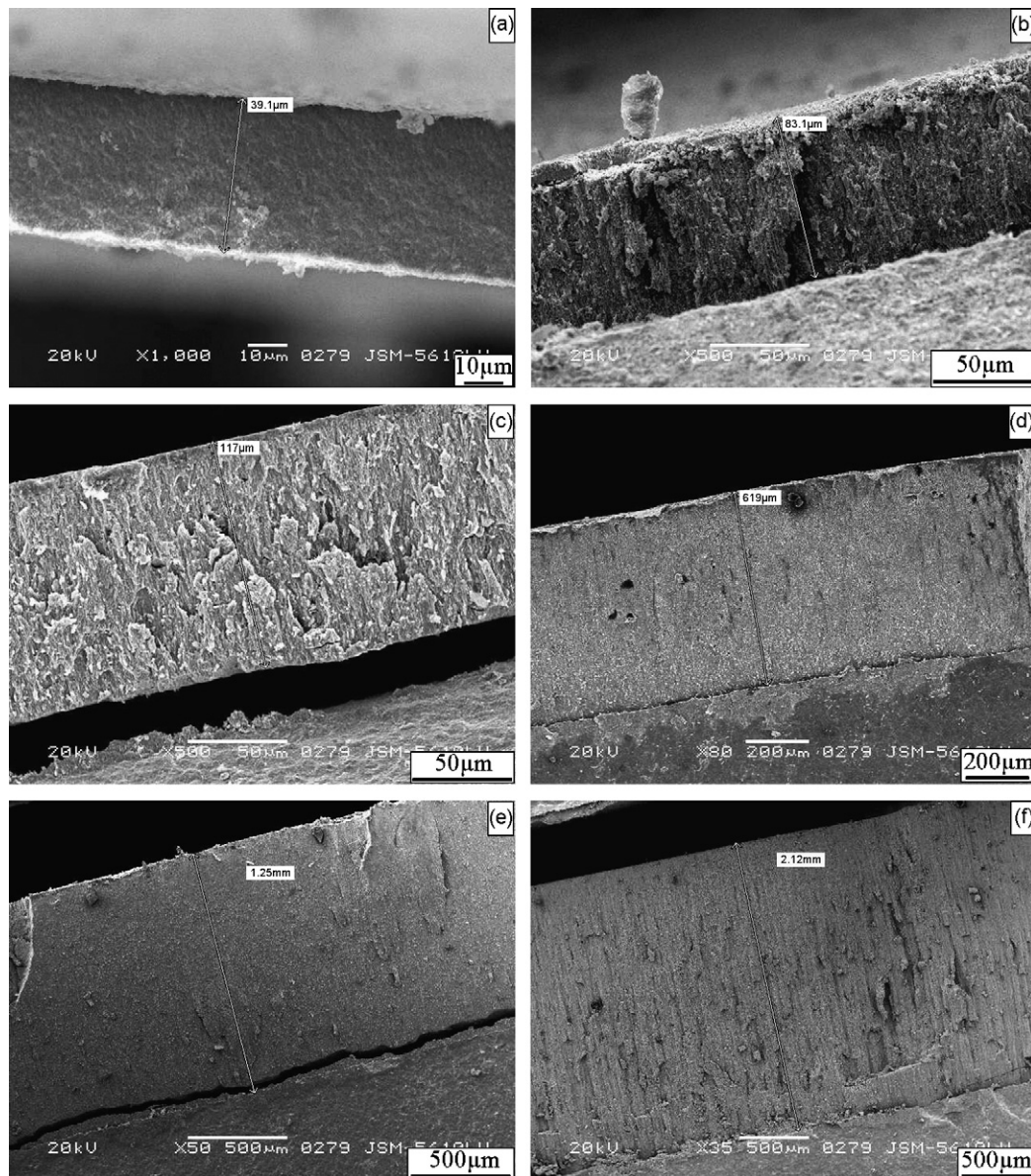


Fig. 3. SEM micrographs of the oxidation layer of specimens oxidized at: (a) 450 °C, (b) 500 °C, (c) 550 °C, (d) 600 °C, (e) 650 °C and (f) 700 °C.

The TRS of the oxidized ultrafine WC–10Co-cemented carbide decreased with increasing oxidation temperature as shown in Fig. 4(a), and the Vickers hardness of specimens measured under a load of 29.4 N also decreased as shown in Fig. 4(b). Although the oxidized surface layer had been removed by polishing, the cobalt and tungsten carbide phases were partly oxidized below the oxidized surface layer, and the microstructure was very loose while large grains were formed. The Vickers hardness was lower than for the polished untreated specimens, because of the defects such as large grains and loose microstructure on the surface of the hardmetals after oxidation. The Vickers hardness HV3 of the sample oxidized at 700 °C was only 1480 kg/mm<sup>2</sup>, which was much lower than 1893 kg/mm<sup>2</sup> of the polished and untreated sample, and the TRS of the sample oxidized at 700 °C was only 839 MPa, which was much lower than the

2230 MPa of the polished and untreated specimen. However, the average value of the Rockwell A hardness was 92.5, which fluctuated a little with the increase of the oxidation temperature.

The Vickers hardness along the cross-section of the sample oxidized at 700 °C was also tested. The Vickers hardness HV3 of the sample near the surface was 1506 kg/mm<sup>2</sup> and 1623 kg/mm<sup>2</sup>, respectively, which was much lower than 1893 kg/mm<sup>2</sup> of the polished and untreated sample. The Vickers hardness near the center of the sample was closer to the Vickers hardness of the polished and untreated sample, as shown in Fig. 5.

As shown in Fig. 6, the saturated magnetization and coercivity force of WC–10Co-cemented carbide decreased with the increase of oxidation temperature, when the oxidation temperature was up to 700 °C, the value of saturated



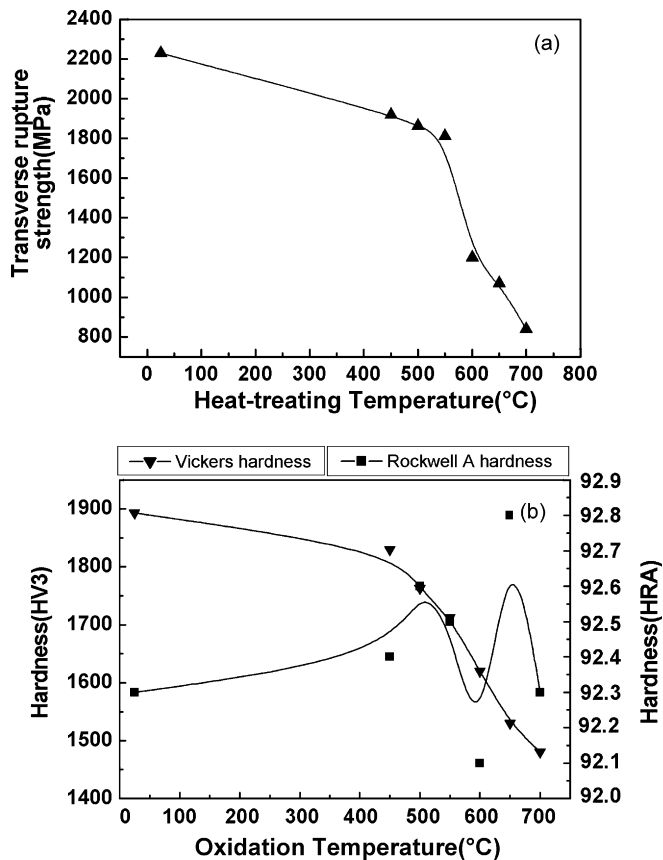


Fig. 4. Variation of (a) TRS, (b) Vickers hardness (HV3) and Rockwell A hardness of ultrafine WC–10Co-cemented carbide as a function of the oxidation temperature.

magnetization and coercivity force were 58% and  $16.5 \text{ kA m}^{-1}$ , respectively. Ultrafine WC–10Co-cemented carbide was decarburized by the oxygen in air, gradually decreasing the saturated magnetization. The high oxidation temperature and atmosphere promoted the fine grain to change to coarse one, so the value of coercivity force decreased gradually. According to the relationship between hardness and bending strength of

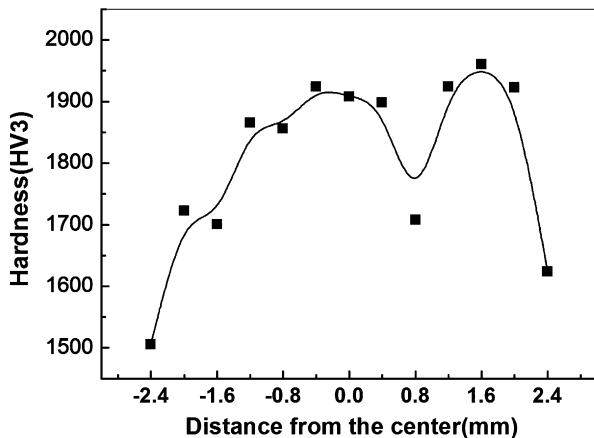


Fig. 5. Vickers hardness (HV3) variation of cross-sectioned of ultrafine WC–10Co-cemented carbide oxidized at 700 °C as a function of the distance from the center of the sample.

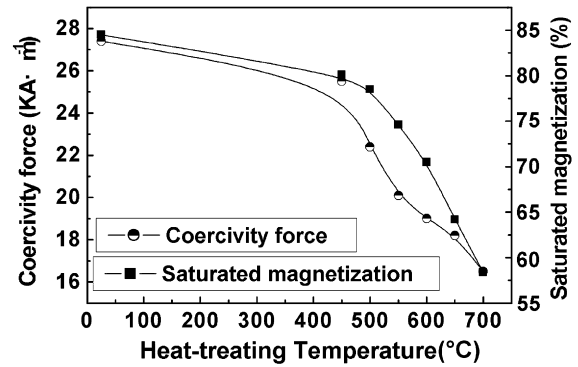


Fig. 6. Variation of saturated magnetization and coercivity force of oxidized ultrafine WC–10Co-cemented carbide with the oxidized temperature.

ultrafine (0.2–0.5  $\mu\text{m}$  WC), submicron (0.5–0.8  $\mu\text{m}$  WC) and fine grain sized (0.8–1.3  $\mu\text{m}$  WC) hardmetals [4], the finer the WC grain size, the higher the hardness and TRS of the ultrafine hardmetals.

Fig. 7 shows optical micrographs of the Vickers indentation on specimens oxidized in air at: (a) 450 °C, (b) 500 °C, (c) 550 °C, (d) 600 °C, (e) 650 °C and (f) 700 °C, respectively. No cracks near the indents were present. Instead, there were a lot of pits on the surfaces of oxidized samples of 450 °C, 500 °C and 550 °C, respectively. The cobalt phase was partly evaporated, Co and WC phases were partly oxidized, and a few WC grains were pulled out during the polishing processes. A lot of larger grains were also observed. Although few pits on the surfaces of oxidized samples of 600 °C, 650 °C and 700 °C were observed, some larger grains were recognized, even the size of a few grains was larger than 10  $\mu\text{m}$ .

As shown in Fig. 8(a), most of the WC grains of the untreated specimen were around 200–400 nm, which was about several times that of the WC grains of the starting nanocomposite powder. Most of the WC grains of the 500 °C oxidized specimen were around 1  $\mu\text{m}$  as shown in Fig. 8(b). In the outer, near surface areas of the sample, where the ultrafine WC–10Co-cemented carbide was in direct contact with the decarburizing atmosphere, there were several large grains with a size up to 3  $\mu\text{m}$ . Most of the WC grains of the 600 °C oxidized ultrafine-cemented carbide were around 1  $\mu\text{m}$  as shown in Fig. 8(c), but there were several large grains whose size was up to 7  $\mu\text{m}$ . The WC grains of the 700 °C oxidized ultrafine-cemented carbide were around 1  $\mu\text{m}$  as shown in Fig. 7(d), but there were several large grains whose size was up to 10  $\mu\text{m}$ .

As shown in Fig. 9(a), the grain size in the oxide layer was smaller than 100 nm, and large grains were not present. Because the oxide layer was loosely attached, the oxide layer broke away from the sample oxidized at 700 °C during the process of obtaining the fractured surface. As shown in Fig. 9(b), near the oxide surface (left), there were a few large grains existing. Far from the oxide surface (right), the grain size seemed to change little. It showed that larger grains existed only in the outer, near surface areas of the sample, where the ultrafine WC–10Co-cemented carbide was in direct contact with the decarburizing oxidizing atmosphere, obviously as a result of the gross carbon content. The oxygen in air reacted

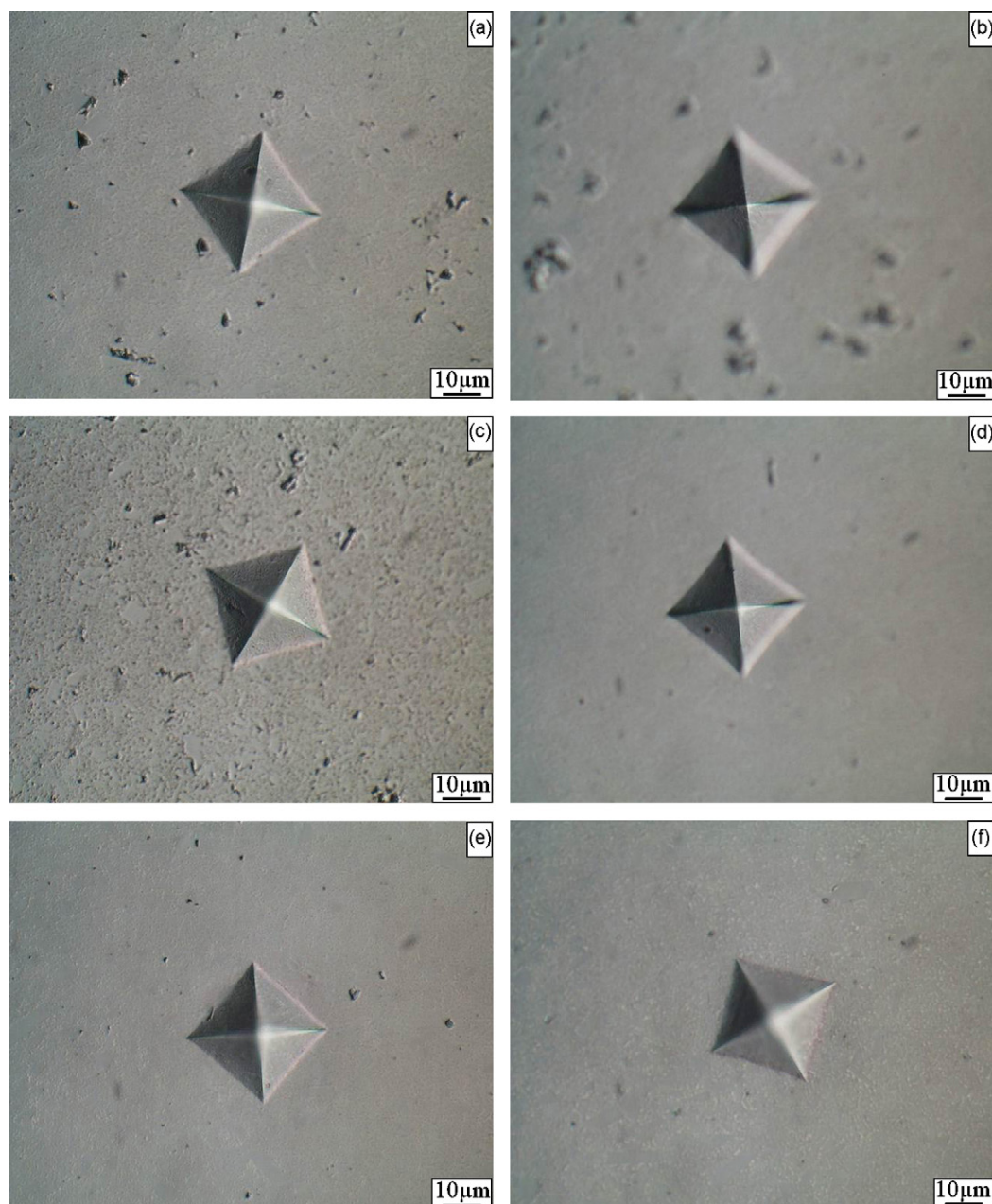
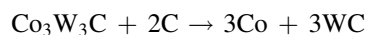


Fig. 7. Optical micrographs of Vickers indentations on specimens after the oxidation processes at: (a) 450 °C, (b) 500 °C, (c) 550 °C, (d) 600 °C, (e) 650 °C and (f) 700 °C.

with WC in the near surface areas of the samples during oxidation at 500–1000 °C forming  $\text{CO}_2$  and  $\text{CO}$ , causing a local carbon deficiency, where eta carbides ( $\text{Co}_3\text{W}_3\text{C}$ ,  $\text{Co}_6\text{W}_6\text{C}$ ) could be formed [14].

As shown in Fig. 10, eta phases  $\text{Co}_6\text{W}_6\text{C}$ ,  $\text{Co}_3\text{W}_3\text{C}$  and  $\text{W}_2\text{C}$  were found in the polished surface of the ultrafine WC–10Co-cemented carbide oxidized at 700 °C. Although subsequent transformation of these carbides could form WC and Co, according to [14]



Carbonizing conditions (by carbon diffusion from carbon-rich areas) might result in the in situ formation of WC and the

formation of large WC grains. An important prerequisite for this formation mechanism is the assumption of non-equilibrium during early sintering (cobalt spreading onto the WC surfaces) and the build-up of carbon activity differences during sintering. The WC particles of spherical shape were homogeneously dispersed in the Co phase in the WC–10Co nanocomposite powder fabricated by spray pyrolysis-continuous reduction and carbonization technology. High-resolution electron microscopy analysis indicated that the single WC crystals were covered by a Co film with thickness of 10–25 nm [1]. After vacuum sintering, cobalt easily spreads onto the WC surface, and little free carbon was retained in the specimens, so the prerequisite for this formation mechanism exists. Moreover, carbon



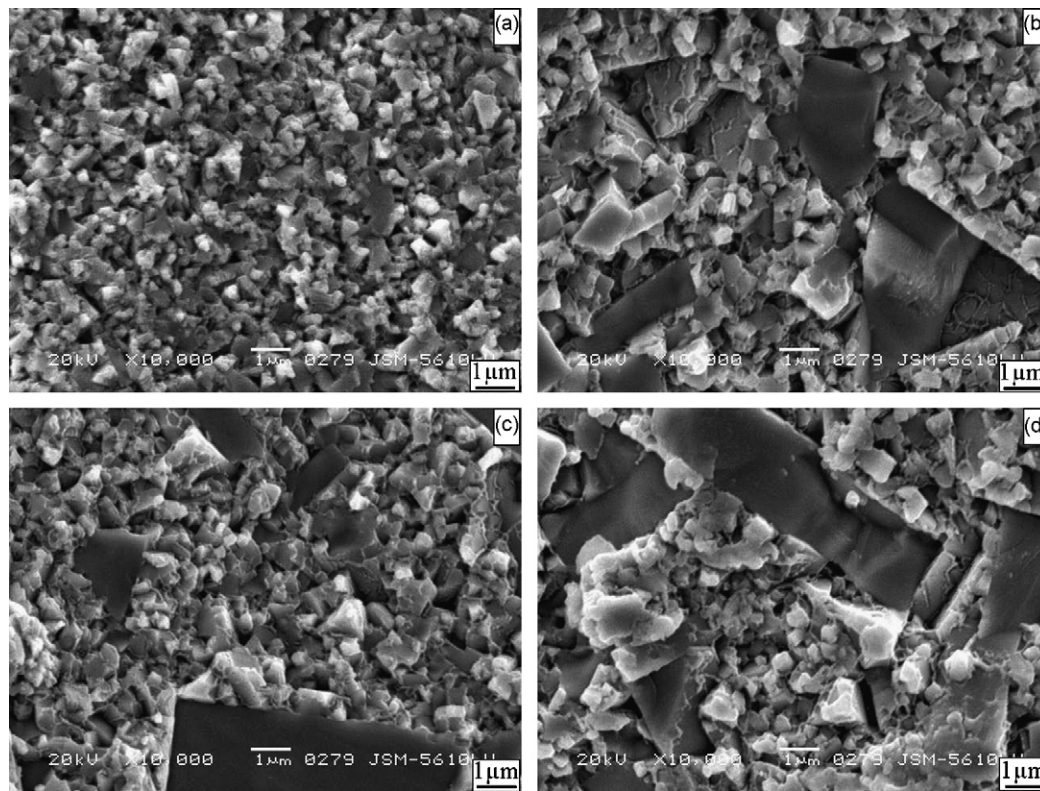


Fig. 8. SEM micrographs of the fractured near surface areas of the samples after oxidation at different temperature: (a) room temperature, (b) 500 °C, (c) 600 °C and (d) 700 °C.

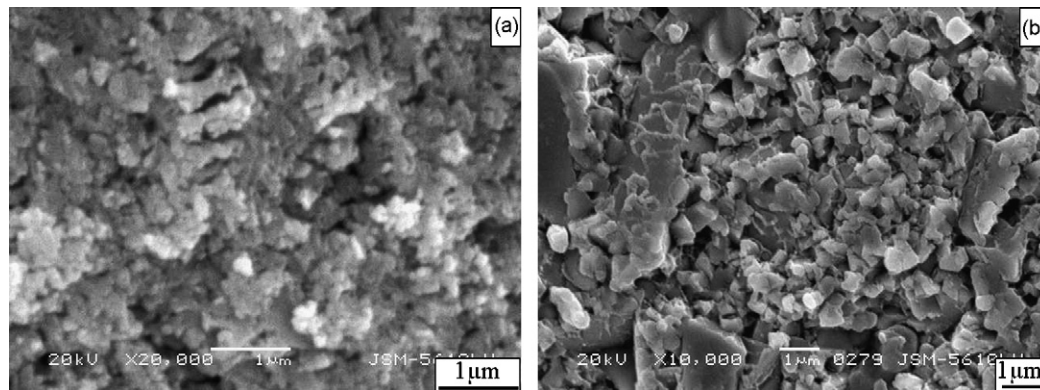


Fig. 9. SEM micrographs of the oxide layer (a) and the cross-sectional view of the interface between the oxide layer and the cemented carbide (b) of ultrafine WC–10Co-cemented carbide oxidized at 700 °C.

diffusion at 500–700 °C is not fast enough to convert such size of eta phase grains into WC within 4 h. So the few large grains might be eta carbides.

As shown in Fig. 4(b), the Vickers hardness of the oxidized samples decreased with increasing of oxidation temperature, but the Rockwell A hardness of the oxidized samples did not decrease and only fluctuated little. As shown in Fig. 5, although the Vickers hardness HV3 along the cross-section of the sample oxidized at 700 °C near the surface was much lower than that of the polished and untreated sample, the Vickers hardness near the center of the sample was closer to the polished and untreated sample. The load for Rockwell A hardness was 490.3 N, which was much larger than the load

29.4 N of the Vickers hardness test. During the process of the Rockwell A hardness testing, the indenter could penetrate through the surface layer with the large grains as shown in Fig. 8, so the Rockwell A hardness of the samples was not affected by the surface layer that was produced by the oxidation process in air. But the load of the Vickers hardness test could not assure the indenter to penetrate through the surface layer, and the Vickers hardness of oxidized ultrafine WC–10Co-cemented carbide decreased with increasing oxidation temperature in air, that is, the Vickers hardness is more superficial than the Rockwell A hardness, revealing that the surface state of the oxidized WC–10Co specimens was not representative for the bulk of the material.

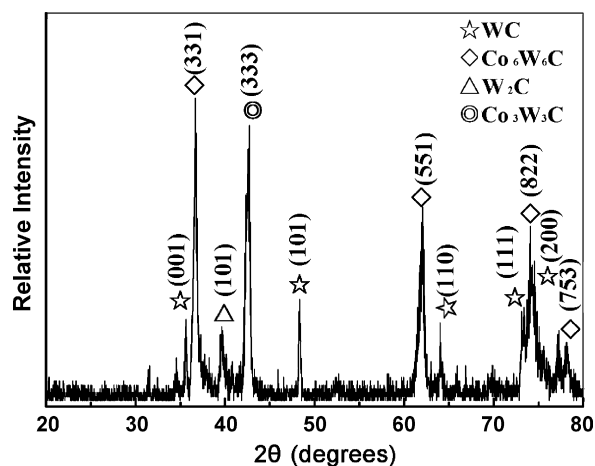


Fig. 10. XRD pattern of the polished surface of the ultrafine WC–10Co-cemented carbide oxidized at 700 °C.

#### 4. Conclusions

The mass increment upon oxidation only changed a little from room temperature to 750 °C, whereas the weight increased greatly from 750 °C to 1000 °C. Ultrafine WC–10Co-cemented carbides oxidized in air at 450 °C, 500 °C, 550 °C, 600 °C, 650 °C and 700 °C for 4 h in a muffle furnace, revealed an oxide layer thickness of 0.04 mm, 0.08 mm, 0.12 mm, 0.62 mm, 1.25 mm and 2.12 mm, respectively. The Vickers hardness and TRS of the specimens after oxide layer removal decreased greatly with increasing oxidation temperature.

#### Acknowledgements

This work was supported by the National Natural Science Foundation of China (50502026), Key Project for Science and

Technology Development of Wuhan city (20041003068-04), and the Key Project for the Sci. & Tech. Research of Chinese Ministry of Education (105123).

#### References

- [1] G.Q. Shao, X.L. Duan, J.R. Xie, et al., Sintering of nanocrystalline WC–Co composite powder, *Rev. Adv. Mater. Sci.* 5 (4) (2003) 281–283.
- [2] G.S. Upadhyaya, Materials science of cemented carbides—an overview, *Mater. Des.* 22 (6) (2001) 483–489.
- [3] A. Upadhyaya, D. Sarathy, G. Wagner, Advances in sintering of hard metals, *Mater. Des.* 22 (6) (2001) 499–506.
- [4] G. Gille, B. Szesny, K. Dreyer, et al., Submicron and ultrafine grained hardmetals for microdrills and metal cutting inserts, *Int. J. Ref. Metal Hard Mater.* 20 (1) (2002) 3–22.
- [5] W.D. Schubert, H. Neumeister, G. Kinger, et al., Hardness to toughness relationship of fine-grained WC–Co hardmetals, *Int. J. Ref. Metal Hard Mater.* 16 (2) (1998) 133–142.
- [6] C.H. Allibert, Sintering features of cemented carbides WC–Co processed from fine powders, *Int. J. Ref. Metal Hard Mater.* 19 (1) (2001) 53–61.
- [7] H.W. Heinrich, D. Schmidt, Intern. Patent C22C.29/08, 06 February, 2003.
- [8] S. Luyckx, High temperature hardness of WC–Co–Ru, *J. Mater. Sci. Lett.* 21 (21) (2002) 1681–1682.
- [9] W.M. Stoll, J.P. Materkowski, T.R. Massa, Intern. Patent C22C.29/00, 29 June, 1996.
- [10] E. Marui, H. Endo, A. Ohira, Wear test of cemented tungsten carbide at high atmospheric temperature (400 °C), *Trib. Lett.* 8 (2–3) (2000) 139–145.
- [11] J.B.J.W. Hegeman, J.T.M. De Hosson, G. de With, Grinding of WC–Co hardmetals, *Wear* 248 (1–2) (2001) 187–196.
- [12] W. Acchar, U.U. Gomes, W.A. Kaysser, et al., Strength degradation of a tungsten carbide–cobalt composite at elevated temperatures, *Mater. Charact.* 43 (1) (1999) 27–32.
- [13] B. Casas, X. Ramis, M. Anglada, et al., Oxidation-induced strength degradation of WC–Co hardmetals, *Int. J. Ref. Metal Hard Mater.* 19 (4–6) (2001) 303–309.
- [14] S.N. Basu, V.K. Sarin, Oxidation behavior of WC–Co, *Mater. Sci. Eng. A* 209 (1–2) (1996) 206–209.
- [15] P.H. Mayrhofer, C. Mitterer, L. Hultman, et al., Microstructural design of hard coatings, *Prog. Mater. Sci.* 51 (8) (2006) 1032–1114.